

# VeriRAG: A Retrieval-Augmented Framework for Automated RTL Testability Repair

Haomin Qi<sup>1,2,†,‡</sup>, Yuyang Du<sup>1,†</sup>, Lihao Zhang<sup>1</sup>, Soung Chang Liew<sup>1,\*</sup>, Kexin Chen<sup>1</sup>, Yining Du<sup>1,3,‡</sup>

<sup>1</sup>The Chinese University of Hong Kong, <sup>2</sup>University of California San Diego, <sup>3</sup>Hong Kong University  
h.chee@link.cuhk.edu.hk, {dy020, zl018, soung}@ie.cuhk.edu.hk, kxchen@cse.cuhk.edu.hk, yiningdu@connect.hku.hk

**Abstract**—Large language models (LLMs) have demonstrated immense potential in computer-aided design (CAD), particularly for automated debugging and verification within electronic design automation (EDA) tools. However, Design for Testability (DFT) remains a relatively underexplored area. This paper presents *VeriRAG*, the first LLM-assisted DFT-EDA framework. *VeriRAG* leverages a Retrieval-Augmented Generation (RAG) approach to enable LLM to revise code to ensure DFT compliance. *VeriRAG* integrates (1) an autoencoder-based similarity measurement model for precise retrieval of reference RTL designs for the LLM, and (2) an iterative code revision pipeline that allows the LLM to ensure DFT compliance while maintaining synthesizability. To support *VeriRAG*, we introduce *VeriDFT*, a Verilog-based DFT dataset curated for DFT-aware RTL repairs. *VeriRAG* retrieves structurally similar RTL designs from *VeriDFT*, each paired with a rigorously validated correction, as references for code repair. With *VeriRAG* and *VeriDFT*, we achieve fully automated DFT correction – resulting in a 7.72-fold improvement in successful repair rate compared to the zero-shot baseline (Fig. 5 in Section V). Ablation studies further confirm the contribution of each component of the *VeriRAG* framework. We open-source our data, models, and scripts at <https://github.com/yuyangdu01/LLM4DFT>.

**Index Terms**—Design for testability, computer-aided design, large language models, retrieval-augmented generation

## I. INTRODUCTION

Recent advancements in large language models (LLMs) have demonstrated significant potential in enhancing computer-aided design (CAD) workflows, particularly in automated debugging and verification of hardware description languages (HDLs) [1, 2]. However, despite the growing interest in LLM-empowered CAD tools, the domain of design for testability (DFT) remains comparatively underexplored.

As systems scale to millions of transistors and face tight timing, yield, and power constraints, addressing testability at the register-transfer level (RTL) stage becomes imperative – resolving DFT issues early enables synthesis tools to optimize area and facilitate reuse without requiring repeated fixes [3, 4]. Moreover, many system-on-chip (SoC) designs integrate IP cores from diverse sources, making RTL-level testability crucial for meeting fault coverage goals and minimizing iterative cycles of synthesis, verification, and automatic test pattern generation (ATPG). In practice, engineers still rely heavily on

time-consuming manual processes to ensure DFT compliance. There is an urgent need for automated approaches to perform DFT-oriented HDL code repairs[5, 6].

We propose *VeriRAG* – a retrieval-augmented generation (RAG) framework for efficient LLM-based RTL repair for DFT compliance – along with an associated DFT dataset named *VeriDFT*. *VeriRAG* incorporates (1) an autoencoder trained by the contrastive learning method to identify DFT-related hardware similarities, and (2) an iterative error correction pipeline guided by compiler diagnostics and DFT error reports. *VeriDFT* is curated from an open-sourced Verilog dataset [7], augmented by our manual annotations to capture classic DFT errors in Verilog HDLs.

Given a Verilog code snippet potentially requiring DFT-compliance code revisions, *VeriRAG* analyzes the hardware structure of the RTL design and retrieves the most similar example from the *VeriDFT* dataset based on both hardware structure and DFT errors. The retrieved example, along with our manually edited solution for DFT compliance, serves as a tailored in-context reference to guide the LLM’s correction of the given Verilog code snippet.

Importantly, *VeriRAG*’s error correction mechanism iteratively refines the RTL design by leveraging compiler diagnostics and DFT error reports generated by electronic design automation (EDA) tools. This iterative process ensures that the modifications effectively address DFT concerns while preserving the design’s synthesizability and logical integrity.

To validate its effectiveness and robustness across diverse language models, we evaluate *VeriRAG* using several state-of-the-art LLMs, including GPT-o1, Grok-3, GPT-4o, Claude-3.7-Sonnet, and Gemini-2.5-Pro. Among these models, GPT-o1 achieves the highest rate of success for DFT error correction – a successful correction is defined as eliminating DFT errors while retaining synthesizability and logical equivalence. Given the inherent complexity of this task, the overall success rate remains modest, with GPT-o1 achieving a 53.76% success rate on the test set. Despite this, the result represents a significant milestone, marking a 7.72-fold improvement over the baseline success rate of 6.96%, achieved by the same LLM using naive prompting strategies (see Fig. 5 in Section V). Comprehensive ablation studies were conducted to validate the necessity of each component within *VeriRAG*.

While the above results highlight the potential of *VeriRAG*, further investigations might be conducted to boost the success rate. First, expanding the *VeriDFT* dataset to include a broader

<sup>†</sup>H. Qi and Y. Du contributed equally to this work.

<sup>‡</sup>Work conducted during internship at IE Department, CUHK.

\*S. C. Liew (soug@ie.cuhk.edu.hk) is the corresponding author.

The work was partially supported by the Shen Zhen-Hong Kong-Macao technical program (Type C) under Grant No. SGDX20230821094359004.

range of DFT error scenarios and RTL design patterns could provide the LLM with more diverse in-context references, thereby improving its ability to generalize to unseen cases. Second, exploring advanced retrieval techniques, such as graph-based methods to capture deeper structural similarities in hardware designs, could further refine the selection of in-context examples. Third, integrating domain-specific pretraining for LLMs on hardware description languages, particularly with a focus on DFT-related tasks, may significantly boost performance by aligning model representations more closely with this specialized domain. Finally, post-training treatments, such as reinforcement learning with automated EDA grading based on fault coverage metrics, could guide the language model for better results.

As an initial effort in the field, this paper makes the following contributions:

- **VeriRAG Framework for DFT-Compliance Code Repair:** We put forth VeriRAG, a RAG-based pipeline that leverages an autoencoder-driven similarity model and an iterative, compiler-guided revision loop to improve LLM performance on DFT-oriented Verilog repair tasks.
- **Domain-Specific Dataset VeriDFT:** To support VeriRAG, we construct VeriDFT, the first RTL design dataset that not only catalogs representative DFT error patterns but also supplies corresponding manually validated corrections for each example. VeriDFT fills a critical gap in hardware testability research, offering high-quality data tailored for DFT-driven retrieval and repair.
- **Benchmarks and Open-Source Contributions:** We conduct extensive evaluations of VeriRAG, establishing the first benchmarking baseline for LLM-based DFT error corrections at the RTL stage. To foster reproducibility and future research, we release all related resources, including (1) the reference implementation of VeriRAG, (2) the VeriDFT dataset, and (3) EDA scripts for compiler diagnostics, DFT error reporting, and logic equivalence check (LEC).

## II. BACKGROUND AND RELATED WORKS

### A. LLM for CAD

LLMs are increasingly being used in CAD, supporting tasks ranging from high-level synthesis to RTL bug detection. Recent studies have shown that LLMs can assist with targeted design improvements, automate documentation, and even interface with EDA tools for power and timing analysis based on user inputs [8, 9, 10, 11, 12, 13]. However, most of these efforts have focused on functional correctness, such as verifying data paths or refining structural descriptions, while largely neglecting the critical aspect of testability. Our work addresses this gap by specifically targeting DFT compliance in RTL designs, broadening the scope of LLM-assisted CAD to include comprehensive testability objectives.

### B. DFT at RTL level

Conventional DFT techniques — such as scan-chain insertion [14], boundary scan [15], and built-in self-test [16]

— primarily operate at the gate level or during physical implementation. While these methods automate many aspects of test generation and reduce manual effort in late design stages, they do not address defects introduced at the RTL stage. Consequently, designers must rely on linting and static analysis tools to identify code-quality issues. The systematic identification and correction of DFT-related errors, particularly those involving internal clocking or asynchronous resets, remains labor-intensive and requires significant expertise [17].

To address these challenges, we propose an LLM-assisted automated framework enabling the detection and correction of critical DFT issues at the RTL level in a fully automatic manner. Our solution enhances testability without compromising design integrity, substantially reducing the need for manual intervention in DFT debugging. In this work, we focus on four representative DFT error types: asynchronous set/reset inaccessible from primary inputs (ACNCPI), internally generated clock domains (CLKNPI), clock used as data (CDFDAT), and flip-flop-driven clocks (FFCKNP).

### C. RAG for RTL design

RAG combines generative modeling with the retrieval of relevant external knowledge to enhance performance. When employing RAG for our purpose, code templates and bug-fix repositories can be leveraged to guide language model outputs, improving both the precision and correctness of LLM-assisted code repairs [18]. For RTL design, previous retrieval-based methods [19] have shown that proactively identifying and reusing well-validated IP and design blocks can significantly improve development efficiency. However, applying RAG to DFT repair introduces a unique challenge: defining and measuring “similarity” for the precise retrieval of the most relevant reference from the knowledge base. To address this, we propose an autoencoder, trained using the contrastive learning method, to quantify DFT-related hardware similarity for effective retrieval within the RAG framework.

### D. Deep Learning for Hardware and DFT Error Analysis

Deep learning has recently become a powerful tool for hardware analysis, achieving notable results in power modeling [20], defect localization [21], and timing optimization [22, 23]. Most existing methods cast hardware analysis as classification or regression tasks, such as anomaly detection, layout optimization, or performance prediction. This paper focuses specifically on the measurement of similarity among RTL designs with DFT defects. We train a supervised autoencoder using contrastive learning to map Verilog files into a latent embedding space that captures their hardware structures and DFT error types. The similarity of two RTL designs is quantified via the cosine similarity between their embedding vectors.

## III. THE VERIDFT DATASET

### A. Data Cleaning and Data partition

Our VeriDFT dataset builds upon a publicly available data collection containing 108,971 Verilog code samples [7]. The

original dataset contains substantial DFT-irrelevant content that may impair the effectiveness of downstream analysis. Comprehensive data cleaning is required. The preprocessing steps outlined below address issues such as non-functional files, extraneous modules, and compilation errors.

First, we filter out Verilog files without meaningful logic functionality, such as testbenches and module wrappers. While these files are essential for simulation, they do not contain circuit designs relevant to DFT analysis. Second, we notice that many designs depend on pre-defined low-level modules or built-in IP cores provided by EDA tools (e.g., Xilinx IP cores in Vivado). Although our EDA tools report errors due to missing IP cores, many of these RTL designs still contain synthesizable logic beyond the instantiation of these unavailable modules. To use such designs in our work, we substitute unavailable IP cores with blank modules with appropriate interfaces to bypass the compilation errors. After that, we compile the Verilog code using Xcelium, employing HAL to generate a customized constraint file for the compilation process.

The EDA compiler validates the synthesizability of RTL logic in each Verilog file, filtering out unsynthesizable designs. Meanwhile, the compiler also provides DFT-related information within the code including (1) the type of each DFT violation in the code, and (2) the specific line in which the DFT violation happens. Only four major types of DFT errors (ACNCPI, CLKNPI, CDFDAT, and FFCKNP, as discussed in the related works) are considered in this paper, while RTL designs containing other DFT error types are excluded from the dataset. For better focus, we also filtered out RTL designs containing multiple types of DFT violations, keeping those with single DFT error only.<sup>1</sup>

We obtained a total of 437 Verilog files with the above process. The proportion of DFT error types and the distribution of code length (in “number of lines”) are given in Fig. 1a and Fig. 1b, respectively.

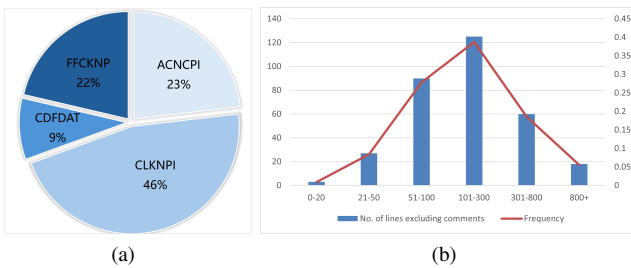


Fig. 1: Statistic overview of the VeriDFT dataset: (a) proportion of DFT-related error types, and (b) code length distribution histogram.

The 437 files in VeriDFT are partitioned as follows. A relatively small training set is used to capture key characterization

<sup>1</sup>As an initial effort in this field, we start from RTL designs with single type of DFT violation within the four critical types. Additional DFT error types, as well as more complex RTL designs with multiple DFT violations will be investigated in future works.

patterns. Most of the designs are reserved for rigorous testing of the framework.

**Training** (see Section IV-A): Approximately 20% (85 files) are used to train the autoencoder network using the contrastive learning approach. These training files are selected to encompass all DFT error types, ensuring the model encountered representative examples of each category.

**Testing** (see Section IV-B): (i) Reference Set – Approximately 8% (35 files) are designated as the reference dataset during testing. Each RTL design in this reference set is paired with a validated revision – the revised version has been compiled with Xcelium and verified by Cadence Conformal LEC to ensure logical equivalence and DFT compliance. This curated set serves as a fixed library of retrieval examples during the RAG code repair process. (ii) Test Set – The remaining 72% of the dataset (317 files) are used as the testing dataset to evaluate the performance of VeriRAG. During testing, an input RTL design from the test set and each reference sample from the reference set are passed through the autoencoder to generate their embedding vectors. The cosine similarity between the two embedding vectors is computed to identify the similarity between the input RTL design and the reference design. After the similarity measurement, the most relevant reference RTL sample, paired with the associated manual revision, is retrieved as the LLM’s RAG reference to revise the given input RTL design to ensure DFT compliance.

### B. Verilog-JSON Conversion to Capture Hardware Similarity

This subsection explains our motivation in using an EDA-generated JSON file for representing the hardware structure in an RTL design and introduces how the Verilog-JSON conversion is conducted.

As the input to the autoencoder network, an RTL design should first be converted into a representation that retains essential information about the circuit’s hardware structure while filtering out irrelevant implementation details. While Verilog codes and design netlists are straightforward representations that allow for textual similarity computations as described in prior works [24, 25], they introduce DFT-irrelevant details that can distract the autoencoder. Specifically, Verilog code contains hardware-irrelevant information such as variable and parameter naming. Design netlists, on the other hand, include excessive low-level hardware details, such as the LUT-based implementation of gates. Fig. 2(b) and Fig. 2(c) give specific examples to illustrate the drawbacks of using Verilog code and design netlists for measuring design similarity.

To obtain the desired RTL representation, we transform Verilog designs into structured JSON files using Yosys, an open-source EDA synthesis tool. As illustrated in Fig. 2(d), these JSON files are derived from netlists and emphasize topological connections among fundamental hardware structures (e.g., combinational/sequential logic, clock/data paths) instead of their implementation details (e.g., how the gate is realized with a look up table). This transformation captures the circuit topology while eliminating extraneous details.

As an important data pre-processing step before the model training and testing, we convert all RTL designs in VeriDFT into their JSON representations.

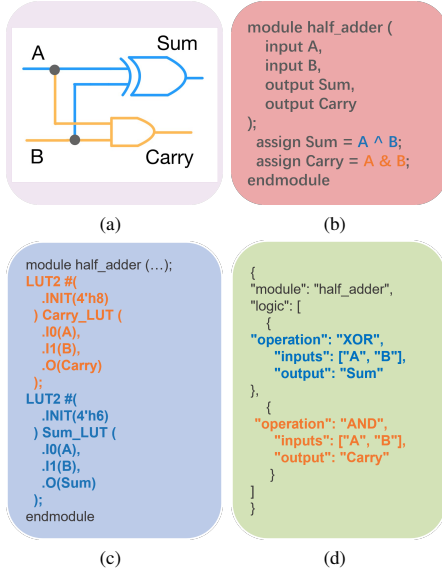


Fig. 2: Verilog-to-JSON transformation: (a) circuit diagram; (b) corresponding RTL implementation; (c) detailed netlist with low-level look up table (LUT) implementation (a distraction for similarity measurement); (d) JSON representation generated by Yosys capturing topological connections between major logic gates and sequential elements. In this work, “hardware structure” refers to these gate-level topologies, reflecting the structural context critical to DFT error patterns.

#### IV. METHODOLOGY

This section presents the implementation of VeriRAG. Fig. 3(a) pertains to the training of the autoencoder, and Fig. 3(b) pertains to the overall application, where the autoencoder is used at the front end to identify the reference RTL design most similar to a given input RTL design. The most-similar reference design provides the reference for the subsequent LLM to perform code repair on the given input RTL design to ensure DFT compliance.

##### A. Training Autoencoder Network

VeriRAG evaluates the similarity of RTL designs on two key aspects: (1) type of DFT violation, and (2) hardware structure. The preceding Section III-A explained how we obtain the DFT-error type labels that denote the type of DFT violation in an RTL design by analyzing the compilation log. Meanwhile, Section III-B detailed how we generate the JSON representation of an RTL design with Yosys.

This section presents the training process for the autoencoder network, which maps an RTL design into a vector representation that intrinsically captures both (1) and (2) aspects of the design. As mentioned in Section III-A, the similarity between two RTL designs is quantified using the cosine similarity of their corresponding vector representations from the autoencoder outputs.

To this end, we train a multi-task encoder-decoder network with the training data in VeriDFT (Fig.3 (a)). First, we vectorize JSON representations and DFT error labels of the RTL designs in the training dataset. For the former, we apply the Term Frequency - Inverse Document Frequency (TF-IDF) vectorization scheme to convert a JSON description into numerical vector  $\mathbf{x}$ . This vectorization method has been proven to be effective for capturing structural patterns in hardware representations [26, 27]. For the implementation of TF-IDF encoder, we use the default smoothing and sublinear term frequency scaling provided by the Python scikit-learn toolbox, and we set  $\mathbf{x}$  to be a 512-dimensional vector. For the latter, we construct a four-dimensional binary vector  $\mathbf{y}$  with a simple label encoding method, using each binary of the vector to denote the existence of one type of DFT error, i.e.,  $y(i) = 0$  means the absence of DFT error type  $\#i$  in the RTL design, while  $y(i) = 1$  means the existence of DFT error type  $\#i$  in the RTL design. Note for the dataset construction in Section III that this paper, as an initial effort in the field, considers RTL designs with a single type of DFT violation, i.e.,  $\mathbf{y}$  is a one-hot vector in essence.

The training process follows the multi-task encoder-decoder training pipeline as in [28], in which an encoder  $f(\cdot)$ , a decoder  $g(\cdot)$ , and a DFT-error classifier  $h(\cdot)$  are optimized together under a single joint loss (see Fig.3 (a) for the inter-connectivities between the encoder, decoder and the classifier).

The overall loss is defined per batch of size  $B$  as the weighted sum of a reconstruction term  $L_1$ , a classification term  $L_2$ , and a contrastive term  $L_3$ . Note that the decoder and classifier serve only as auxiliary supervisors to ensure the encoder performs good feature mappings in its vectorization process. Therefore, this paper does not present the training details of decoder and classifier. We refer interested readers to Section III of [29] for a detailed introduction of the individual loss components used for decoder and classifier. Before presenting the overall loss function, we first elaborate on the three loss terms within the loss function below:

For the  $k^{\text{th}}$  sample of batched inputs, the encoder takes the 512-dimensional numerical vector  $\mathbf{x}_k$  as input and generates a 128-dimensional embedding vector output  $\mathbf{z}_k$ , i.e.,  $\mathbf{z}_k = f(\mathbf{x}_k)$ . The decoder takes  $\mathbf{z}_k$  as input and generates the reconstructed vector  $\hat{\mathbf{x}}_k$ , i.e.,  $\hat{\mathbf{x}}_k = g(\mathbf{z}_k)$ . The Mean Squared Error (MSE) reconstruction loss  $L_1$  ensures that the embedding vector faithfully preserves all details within the input JSON representation:

$$L_1 = \frac{1}{B} \sum_{k=1}^B \|\mathbf{x}_k - \hat{\mathbf{x}}_k\|_2^2 \quad (1)$$

We also want the encoder output  $\mathbf{z}_k$  to capture the feature about the DFT error violation within the associated RTL design. To this end, we introduce the classification loss term in the general loss function. Specifically,  $\mathbf{z}_k$  is fed to a classification network implemented with a fully connected layer. The output of the classification network is a 4-dimensional vector  $\mathbf{c}_k = h(\mathbf{z}_k)$ . The classification loss term  $L_2$  is defined as the

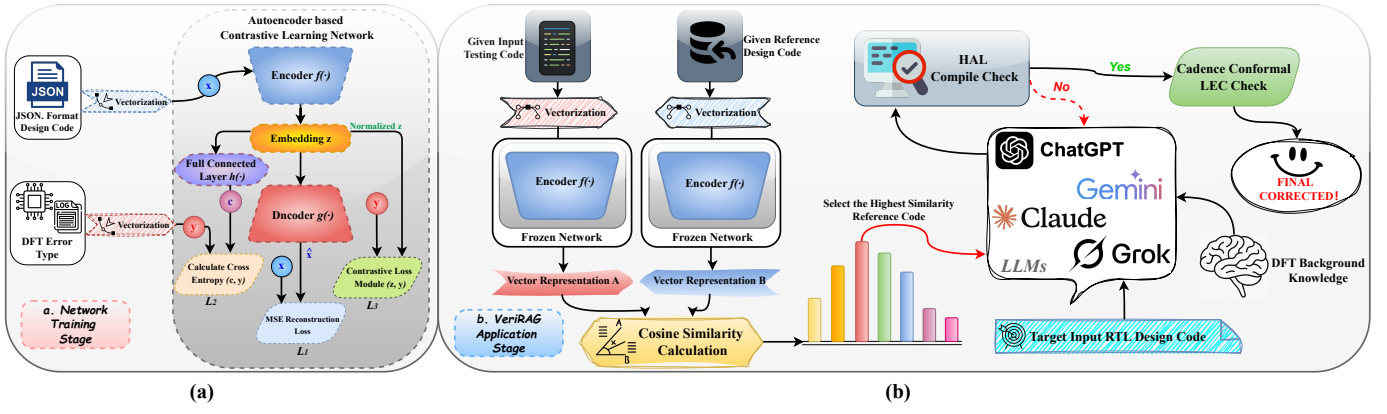


Fig. 3: The VeriRAG framework – (a) training of autoencoder network, (b) RAG-based code revision pipeline in the testing process.

cross entropy between  $c_k$  and the associated DFT error label  $y_k$ , computed per sample and averaged across the same batch of size:

$$\mathcal{L}_2 = -\frac{1}{B} \sum_{k=1}^B \sum_{i=1}^4 y_k(i) \log P_k(i) \quad (2)$$

where  $\mathbf{P}_k$  is the post-softmax probability vector, and  $P_k(i)$  can be written as:

$$P_k(i) = \frac{\exp(c_k(i))}{\sum_{j=1}^4 \exp(c_k(j))} \quad (3)$$

We further introduce a contrastive term in the loss function to encourage embeddings of similar DFT error labels to be closer while pushing those with significantly different labels apart so that RTL designs with the same DFT error types are likely to have embedding high similarity measure, and vice versa. Following the classic setup in [28], given a batch of normalized embeddings  $\{\mathbf{z}_k^{\text{norm}}\}_{k=1}^B$ , in which we have  $\mathbf{z}_k^{\text{norm}} = \mathbf{z}_k / \|\mathbf{z}_k\|$ , and the associated batch of label vector  $\{y_k\}_{k=1}^B$ , we have:

$$\mathcal{L}_3 = \frac{1}{N} \sum_{p < q} \begin{cases} \|\mathbf{z}_p^{\text{norm}} - \mathbf{z}_q^{\text{norm}}\|^2, & y_p = y_q \\ [\max(m - \|\mathbf{z}_p^{\text{norm}} - \mathbf{z}_q^{\text{norm}}\|, 0)]^2, & y_p \neq y_q \end{cases} \quad (4)$$

where  $m$  is a hyperparameter representing the fixed margin, describing the targeted minimum distance between two normalized embedding pairs with different labels.  $N$  denotes the total number of unique unordered sample-pairs in the batch, i.e.  $N = B(B-1)/2$ .

Finally, with the above background, we give the expression of the loss function as

$$\mathcal{L} = \mathcal{L}_1 + \alpha \mathcal{L}_2 + \beta \mathcal{L}_3 \quad (5)$$

where we have  $\alpha = 0.01$  and  $\beta = 0.01$  in our implementation.

### B. Application of VeriRAG framework

The above training process ensures that the encoder network can well identify the hardware structure and DFT violation of a given RTL design input and properly encodes the above

information into the embedding vector. This subsection concerns the application of the encoder in the overall VeriRAG framework.

Given the JSON representation of an input RTL design, denote the associated embedding vector generated by the encoder network by  $\mathbf{z}^T$ , where the superscript  $T$  indicates that this is a testing input. Further, denote the embedding vector for reference RTL design  $r$  in the reference dataset by  $\mathbf{z}_r^R$ , where the superscript  $R$  indicates that this is a reference sample. The similarity between the given RTL design and reference RTL design  $r$ , denoted as  $s_r$ , is defined as the cosine similarity between  $\mathbf{z}^T$  and  $\mathbf{z}_r^R$ , i.e.,

$$s_r = \frac{\mathbf{z}^T \cdot \mathbf{z}_r^R}{\|\mathbf{z}^T\| \|\mathbf{z}_r^R\|}, \quad \text{where } \mathbf{z}^T = f(\mathbf{x}^T), \mathbf{z}_r^R = f(\mathbf{x}_r^R) \quad (6)$$

After comparing the input RTL design and all reference RTL designs in the reference dataset, we obtain a vector of similarity score, i.e.,  $\mathbf{s} = \langle s_1, s_2, \dots, s_n \rangle$ , where  $n$  is the number of reference RTL designs within the reference dataset. By traversing this similarity vector  $\mathbf{s}$ , we select the reference RTL design with the highest similarity score ( $s_{\max}$ ) as the most relevant reference. We refer to the combination of this reference design and its manually edited revision as the “reference-answer pair”.

The VeriRAG framework leverages this reference-answer pair retrieved from the reference dataset to iteratively refine the target input Verilog code. Along with the reference-answer pair, the initial prompt given to the LLM – which is responsible for generating the DFT-compliance code – also contains (1) a general description of the task, (2) a background introduction on testability principles in RTL design, and (3) detailed definitions of the four DFT error types being considered.

Using these prompt inputs, the LLM generates an initial fix for the target Verilog code. To ensure the revised Verilog code is compilable and DFT-compliant, we introduce a feedback loop to check the synthesizability and DFT violation of the resulting design. If any compilation error or DFT violation is found by the EDA compiler (Xcelium, in our implementation), the compilation log will be provided to the LLM, which uses this feedback to refine the code in the next iteration. This

process continues until a successful compilation is achieved or the maximum number of iterations ( $K$ , set to 5 in our implementation) is reached.

Once a successful revision passes the compilation check, it undergoes a final Cadence Conformal Logic Equivalence Check (LEC) to validate logical equivalence. Upon passing this rigorous validation, the RTL design is marked as correctly revised, concluding a successful iterative revision process.

## V. EXPERIMENTS

This section evaluates VeriRAG by comparing it against three ablation variants described below. The goal of these experiments is to assess the contribution of each component within VeriRAG to the DFT error correction.

**Zero Shot:** The tested LLM receives only the target Verilog file containing DFT errors without any hints – no background information or RTL design references are included in the prompt. This straightforward baseline measures the generic LLM’s ability to handle DFT errors in a single inference step without iterative feedback and error correction.

**No RAG:** In addition to the RTL design requiring revision, the LLM is provided with general DFT knowledge and brief descriptions of the four specific DFT error types. This background information allows the LLM to better understand the task. However, no reference RTL design or iterative refinement process is involved.

**Random RAG:** Along with the general DFT background, the LLM is given a Verilog sample randomly selected from the reference dataset, paired with its corresponding revision. The random reference design may not match the structure or error type of the target RTL design. We adopted the aforementioned iterative revision policy for Random RAG: for fairness, both VeriRAG and Random RAG are allowed up to five error-correction attempts. In each iteration, the LLM receives the most recent corrected version of the RTL (from the previous round), along with its compiler diagnostics. Although the reference sample remains unchanged, the input context evolves iteratively based on the updated design and feedback, enabling progressive refinement over iterations. This is the case for both Random RAG and VeriRAG. The only difference between this baseline and our method is in the retrieval policy – VeriRAG uses the autoencoder to select the most relevant example, while Random RAG selects references randomly.

As mentioned in Section III, the VeriDFT dataset comprises 35 reference RTL designs (each paired with a standard revision) and 317 test files. In the following experiments, we tested all RTL designs in the testing dataset to enable comprehensive assessment using the reference dataset as the retrieval knowledge base. Our experiments focus on two main questions: (1) What proportion of the generated RTL revisions can fully eliminate DFT error while remaining synthesizable? (2) Among those revisions satisfying (1), what proportion also preserves logical equivalence with the original design?

Here, (2) is a subset of (1). Both DFT error elimination and synthesizability in (1) are verified by the compiler, so we consider them together. The rest of this section addresses

these questions by testing five state-of-the-art LLMs: GPT-o1, GPT-4o, Grok-3, Claude-3.7-Sonnet, and Gemini-2.5-Pro.

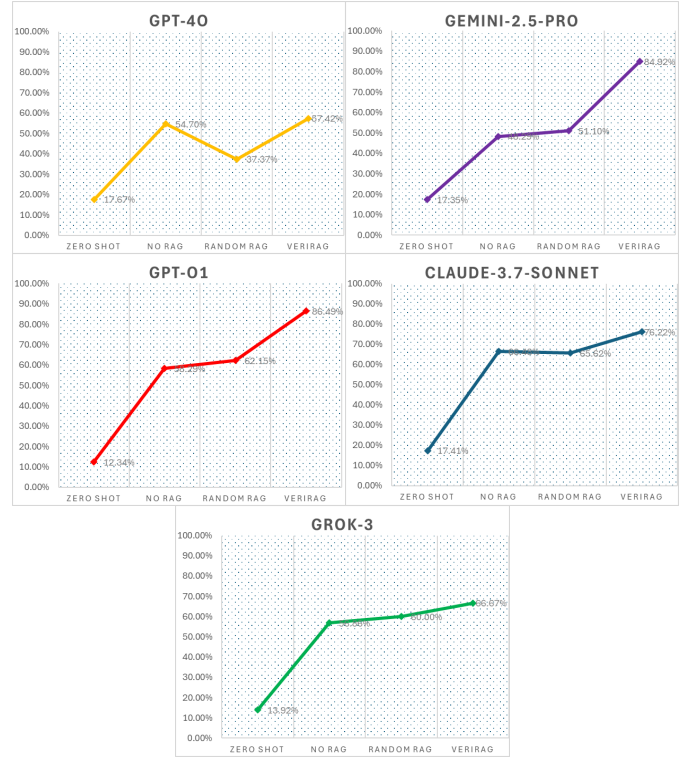


Fig. 4: Success rates of preliminary DFT error corrections (without considering logical equivalence) for different LLMs and ablation cases tested .

We next present experimental results for the tested LLMs under different prompting approaches. Given the test dataset, let  $ANS$  be the total number of RTL revisions generated. Let  $NoErr$  denote the number of RTL revisions that are both free of DFT errors and remain synthesizable, corresponding to question (1) but not (2). Fig. 4 shows the preliminary DFT error correction rate ( $NoErr/ANS$ ) across different LLMs and ablation variants. For these error-free RTL revisions, we further conducted LEC. Let  $Eq$  be the number of logically equivalent RTL designs, corresponding to satisfying both question (1) and (2). Fig. 5 presents the ultimate success rate ( $Eq/ANS$ ) for different LLMs and all ablation cases.

Three key trends are evident across these experimental results. First, the incremental integration of domain-specific context and structured references consistently improves the LLM’s abilities to correct DFT errors. Transitioning from a Zero Shot setting to the advanced VeriRAG configuration increases the ultimate success rates for all tested LLMs. These findings support our central thesis: precise, structure-aware RTL references, combined with the iterative code revision pipeline, significantly outperform generic textual prompts or random reference examples.

Second, the results reveal notable variation in how different LLMs utilize incremental guidance. Grok-3 achieves the largest relative gain, indicating its superior utilization of

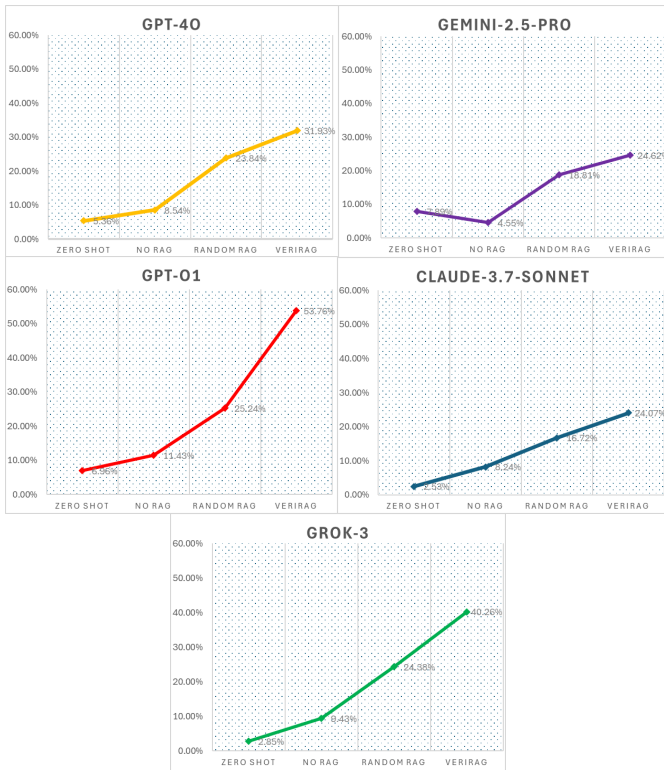


Fig. 5: Ultimate code revision success rates (with logical equivalence) for different LLMs and ablation cases tested.

structural references and iterative feedback, with its logic equivalence rate rising from a minimal 2.85% with Zero Shot to 40.26% with VeriRAG. GPT-4o also benefits markedly, reaching 31.93% equivalence, while Claude-3.7-Sonnet and Gemini-2.5-Pro plateau in the mid-20% range. These results highlight that general purpose LLMs differ significantly in their intrinsic abilities to integrate structured references and iterative compiler feedback into effective RTL corrections.

Finally, GPT-o1 provides a meaningful upper-bound reference, clearly illustrating the potential of large-scale, general-purpose LLMs in the VeriRAG framework. It achieves an ultimate success rate of 53.76%, a 7.72-fold improvement over its Zero Shot baseline. This impressive margin emphasizes the variable win achieved with enhanced structural retrieval and precise compiler-guided iterations, even without domain-specific tuning.

## VI. CONCLUSIONS AND OUTLOOK

We present *VeriRAG*, a retrieval-augmented framework designed to tackle DFT error repair at the RTL stage. This framework employs an autoencoder network trained by contrastive learning to identify and retrieve structurally similar reference code from a newly developed Verilog DFT dataset, referred to as *VeriDFT*. Using the retrieved reference RTL designs, an LLM performs DFT error repairs through an iterative Verilog code revision pipeline. This iterative code-revision process, guided by compiler diagnostics, ensures accurate and reliable error correction.

On a benchmark of 317 tested RTL designs, VeriRAG improves the success rate of DFT repairs by different state-of-the-art LLM models: e.g., from 3% to 40.26% with Grok-3, and from 6.96% to 53.76% with GPT-o1 (13.42-fold and 7.2-fold improvements, respectively). Ablation studies validate the effectiveness of our two key technical contributions: (1) the hardware and DFT similarity-based retrieval scheme, and (2) the iterative code revision pipeline guided by compiler feedback.

There are several promising directions for future work. One open problem revealed in our experiments is the gap between the preliminary success rate and the ultimate success rate. This gap indicates that all these tested LLMs are struggling with writing logically equivalent Verilog codes. This is probably due to these LLMs’ inability to understand subtle circuit design details within these RTL files. We see three avenues to close this gap. First, LLMs fine-tuned, or even pre-trained in the ideal case, on Verilog datasets may attain foundational understanding of hardware structure, hierarchy, and test logic from the massive training data. Second, embedding a lightweight formal-equivalence oracle – e.g., a SAT/SEC engine or incremental LEC – into each repair iteration, turning logical discrepancies into explicit feedback for the LLM. Such “formal-in-the-loop” guidance can bridge the reasoning shortfall without incurring prohibitive runtime overhead and substantially narrow the preliminary-to-ultimate performance gap. Third, our present flow vectorizes from Verilog to JSON may introduce information loss in terms of the hardware’s logical design. A learnable vectorizer/de-vectorizer jointly trained within the network training pipeline – augmented with logic-level signals and equivalence-preserving constraints – could better improve downstream retrieval and repair quality.

On the data side, future work could further enrich VeriDFT. We intend to include more types of DFT violations in VeriDFT and introduce more complex RTL designs with multiple types of DFT errors. Furthermore, future research can strengthen the coverage of the reference dataset in terms of number and diversity by adding more manually edited RTL examples, which can refine the granularity of the retrieval process and result in more reliable DFT error repairs.

## REFERENCES

- [1] J. Blocklove, S. Garg, R. Karri, and H. Pearce, “Evaluating llms for hardware design and test,” in *2024 IEEE LLM Aided Design Workshop (LAD)*. IEEE, 2024, pp. 1–6.
- [2] F. Firouzi, D. Z. Pan, J. Gu, B. Farahani, J. Chaudhuri, Z. Yin, P. Ma, P. Domanski, and K. Chakrabarty, “Chipmnd: Llms for agile chip design,” in *2025 IEEE 43rd VLSI Test Symposium (VTS)*. IEEE, 2025, pp. 1–10.
- [3] L.-T. Wang, C.-W. Wu, and X. Wen, *VLSI test principles and architectures: design for testability*. Elsevier, 2006.
- [4] G. Thakur, S. Jain, and H. Sohal, “Current issues and emerging techniques for vlsi testing-a review,” *Measurement: Sensors*, vol. 24, p. 100497, 2022.

- [5] S. Alsaqer, S. Alajmi, I. Ahmad, and M. Alfaiakawi, "The potential of llms in hardware design," *Journal of Engineering Research*, 2024.
- [6] M. Abdollahi, S. F. Yeganli, M. A. Baharloo, and A. Baniasadi, "Hardware design and verification with large language models: A literature survey, challenges, and open issues," 2024.
- [7] S. Thakur, B. Ahmad, Z. Fan, H. Pearce, B. Tan, R. Karri, B. Dolan-Gavitt, and S. Garg, "Benchmarking large language models for automated Verilog RTL code generation," in *2023 Design, Automation and Test in Europe Conference and Exhibition (DATE)*, 2023, pp. 1–6.
- [8] J. Blocklove, S. Garg, R. Karri, and H. Pearce, "Chip-Chat: Challenges and opportunities in conversational hardware design," in *2023 ACM/IEEE 5th Workshop on Machine Learning for CAD (MLCAD)*, 2023, pp. 1–6.
- [9] M. Liu, N. Pinckney, B. Khailany, and H. Ren, "VerilogEval: Evaluating large language models for Verilog code generation," in *2023 IEEE/ACM International Conference on Computer Aided Design (ICCAD)*, 2023, pp. 1–8.
- [10] Y. Liu, C. Xu, Y. Zhou, Z. Li, and Q. Xu, "Deep-RTL: Bridging verilog understanding and generation with a unified representation model," *arXiv preprint arXiv:2502.15832*, 2025.
- [11] Y. Zhao, D. Huang, C. Li, P. Jin, M. Song, Y. Xu, Z. Nan, M. Gao, T. Ma, L. Qi *et al.*, "CodeV: Empowering LLMs with HDL generation through multi-level summarization," *arXiv preprint arXiv:2407.10424*, 2024.
- [12] Y. Du, H. Deng, S. C. Liew, Y. Shao, K. Chen, and H. Chen, "LLM for complex signal processing in FPGA-based software defined radios: A case study on FFT," in *2024 IEEE 100th Vehicular Technology Conference (VTC2024-Fall)*, 2024, pp. 1–6.
- [13] S. Thakur, B. Ahmad, H. Pearce, B. Tan, B. Dolan-Gavitt, R. Karri, and S. Garg, "Verigen: A large language model for Verilog code generation," *ACM Transactions on Design Automation of Electronic Systems*, vol. 29, no. 3, pp. 1–31, 2024.
- [14] W. Wang, J. Wang, W. Wang, P. Liu, and S. Cai, "A secure DFT architecture protecting crypto chips against scan-based attacks," *IEEE Access*, vol. 7, pp. 22 206–22 213, 2019.
- [15] R. Barr, C.-H. Chiang, and E. Wallace, "End-to-end testing for boards and systems using boundary scan," in *Proceedings International Test Conference 2000 (IEEE Cat. No.00CH37159)*, 2000, pp. 585–592.
- [16] H. Nagle, S. Roy, C. Hawkins, M. McNamer, and R. Fritzscheier, "Design for testability and built-in self test: a review," *IEEE Transactions on Industrial Electronics*, vol. 36, no. 2, pp. 129–140, 1989.
- [17] S. Harrison, P. Collins, and G. Noeninckx, "The implementation of ieee std 1149.1 boundary scan test strategy within a cellular infrastructure production environment," in *Proceedings International Test Conference 2000 (IEEE Cat. No.00CH37159)*, 2000, pp. 45–54.
- [18] P. Lewis, E. Perez, A. Piktus, F. Petroni, V. Karpukhin, N. Goyal, H. Küttler, M. Lewis, W.-t. Yih, T. Rocktäschel *et al.*, "Retrieval-augmented generation for knowledge-intensive NLP tasks," *Advances in neural information processing systems*, vol. 33, pp. 9459–9474, 2020.
- [19] Y.-S. Kung, T.-W. Tsui, and N.-H. Shieh, "Design and implementation of a motion controller for XYZ table based on multiprocessor SoPC," in *2009 Chinese Control and Decision Conference*, 2009, pp. 241–246.
- [20] A. Bhattacharya and S. G. Cloutier, "End-to-end deep learning framework for printed circuit board manufacturing defect classification," *Scientific reports*, vol. 12, no. 1, p. 12559, 2022.
- [21] X. Wang, S. Gao, J. Guo, C. Wang, L. Xiong, and Y. Zou, "Deep learning-based integrated circuit surface defect detection: Addressing information density imbalance for industrial application," *International Journal of Computational Intelligence Systems*, vol. 17, no. 1, p. 29, 2024.
- [22] Z. Guo, M. Liu, J. Gu, S. Zhang, D. Z. Pan, and Y. Lin, "A timing engine inspired graph neural network model for pre-routing slack prediction," in *Proceedings of the 59th ACM/IEEE Design Automation Conference*, 2022, pp. 1207–1212.
- [23] N. Sivakumar, N. Suresh, and G. Arapana, "A deep learning based power estimations mechanism for CMOS VLSI circuit," *ICTACT Journal on Microelectronics*, vol. 8, no. 4, pp. 1471–1475, 2023.
- [24] C. K. Roy and J. R. Cordy, "A survey on software clone detection research," *Queen's School of computing TR*, vol. 541, no. 115, pp. 64–68, 2007.
- [25] M. Mondal, C. K. Roy, and K. A. Schneider, "A survey on clone refactoring and tracking," *Journal of Systems and Software*, vol. 159, p. 110429, 2020.
- [26] S. Thakur, B. Ahmad, Z. Fan, H. Pearce, B. Tan, R. Karri, B. Dolan-Gavitt, and S. Garg, "Benchmarking large language models for automated verilog rtl code generation," in *2023 Design, Automation & Test in Europe Conference & Exhibition (DATE)*. IEEE, 2023, pp. 1–6.
- [27] K. Chen, J. Li, K. Wang, Y. Du, J. Yu, J. Lu, L. Li, J. Qiu, J. Pan, Y. Huang *et al.*, "Chemist-X: large language model-empowered agent for reaction condition recommendation in chemical synthesis," *arXiv preprint arXiv:2311.10776*, 2023.
- [28] P. Khosla, P. Teterwak, C. Wang, A. Sarna, Y. Tian, P. Isola, A. Maschinot, C. Liu, and D. Krishnan, "Supervised contrastive learning," *Advances in neural information processing systems*, vol. 33, pp. 18 661–18 673, 2020.
- [29] J. Aneja, A. Schwing, J. Kautz, and A. Vahdat, "A contrastive learning approach for training variational autoencoder priors," *Advances in neural information processing systems*, vol. 34, pp. 480–493, 2021.